To be submitted to *Journal of Geophysical Research*

Observations of Solar Spectral Irradiance Change During Cycle 22 from NOAA-9 SBUV/2

Matthew T. DeLand, Richard P. Cebula
Science Systems and Applications, Inc. (SSAI)
10210 Greenbelt Road, Suite 400, Lanham, MD 20706 USA

Ernest Hilsenrath
NASA/Goddard Space Flight Center, Code 916
Greenbelt, MD 20771 USA

Abstract. The NOAA-9 Solar Backscatter Ultraviolet, model 2 (SBUV/2) instrument is one of a series of instruments providing daily solar spectral irradiance measurements in the middle and near ultraviolet since 1978. The SBUV/2 instruments are primarily designed to measure stratospheric profile and total column ozone, using the directional albedo as the input to the ozone processing algorithm. As a result, the SBUV/2 instrument does not have onboard monitoring of all time-dependent response changes. We have applied internal comparisons and vicarious (external) comparisons to determine the long-term instrument characterization for NOAA-9 SBUV/2 to derive accurate solar spectral irradiances from March 1985 to May 1997 spanning two solar cycle minima with a single instrument. The NOAA-9 data show an amplitude of 9.3(±2.3)% (81-day averaged) at 200-205 nm for solar cycle 22. This is consistent with the result of $\Delta F_{200\text{-}205}$ = 8.3(±2.6)% for cycle 21 from Nimbus-7 SBUV and $\Delta F_{200\text{-}205}$ = 10(±2)% (daily values) for cycle 23 from UARS SUSIM. NOAA-9 data at 245-250 nm show a solar cycle amplitude of $\Delta F_{245\text{-}250}$ = 5.7(±1.8)%. NOAA-9 SBUV/2 data can be combined with other instruments to create a 25-year record of solar UV irradiance.

1. Introduction

Solar ultraviolet (UV) irradiance is the primary energy source for the Earth's middle atmosphere, with most of the radiation in the wavelength range 190-300 nm deposited between 30-50 km [*Meier*, 1991]. Recent papers discussing solar influences on the middle atmosphere include the following topics: ozone [*Hood*, 1999; *Hood and Zhou*, 1999; *Zhou et al.*, 2000], OH [*Canty and Minschwaner*, 2002], NO_y [*Callis et al.*, 2000], tropospheric ozone [*Chandra et al.*, 1999], dynamics [*Arnold and Robinson*, 1998; *Kodera and Kuroda*, 2002], temperatures and geopotential heights [*van Loon and Shea*, 2000], and models [*Haigh*, 1999; *Balachandran et al.*, 1999; *Shindell et al.*, 1999; *Khosravi et al.*, 2002; *Lee and Smith*, 2003]. Early satellite experiments clearly identified UV irradiance variations with an approximate 27-day period [*Heath*, 1969; *Prag and Morse*, 1970], caused by rotation of active regions across the solar disk. Extended measurements in the 1970s suggested that long-term UV irradiance variations were also present, but differed considerably in estimates of magnitude and spectral dependence [*Smith and Gottlieb*, 1974; *Heath and Thekaekara*, 1977]. Figure 1 shows that beginning in 1978, a series of different satellite instruments have made continuous solar observations over most of the 120-

400 nm wavelength region. Nimbus-7 Solar Backscatter Ultraviolet (SBUV) measured solar activity from solar cycle 21 maximum to the minimum between cycles 21 and 22. Instrument response changes were modeled based on special measurement results from selected periods, but were not measured directly [*Schlesinger and Cebula*, 1992; *DeLand and Cebula*, 2001]. The Solar Mesosphere Explorer (SME) also measured from cycle 21 maximum to the cycle 21-22 minimum. Its long-term calibration was established using multiple solar diffusers and comparisons with rocket underflights [*Rottman*, 1988]. The NOAA-11 SBUV, model 2 (SBUV/2) instrument measured the maximum and declining phase of solar cycle 22. Its long-term calibration utilized an onboard system and comparisons with coincident Shuttle SBUV (SSBUV) measurements from Shuttle flights [*Cebula et al.*, 1998a]. The Upper Atmospheric Research Satellite (UARS) Solar Ultraviolet Spectral Irradiance Monitor (SUSIM) [*Floyd et al.*, 2002] and UARS Solar Stellar Intercomparison Experiment (SOLSTICE) [*Rottman et al.*, 2001] instruments have observed the Sun from the maximum of solar cycle 22 to the maximum of solar cycle 23. SUSIM uses multiple gratings, filters, and detectors in different combinations with onboard deuterium lamps to determine instrument response changes. Both instruments thus rely on their own measurements to derive a complete instrument characterization and produce fully calibrated irradiance data.

The NOAA-9 SBUV/2 instrument was the first in a series of eight instruments designed to continue the Nimbus-7 SBUV measurements from NOAA operational spacecraft. NOAA-9 measured solar spectral UV irradiance from March 1985 to May 1997, providing the first solar irradiance data set covering a complete solar cycle from one minimum to the next. Previous work has examined short-term solar variability during solar minima from the uncorrected NOAA-9 irradiance data [*DeLand and Cebula*, 1998a]. This paper describes the creation of a fully calibrated irradiance data set for NOAA-9 SBUV/2. Estimates of solar cycle amplitude at different UV wavelengths are compared with results from other instruments for the three solar cycles observed to date. The calibrated NOAA-9 data provide the final component needed as input to produce a continuous 25-year data set of solar UV irradiance between 170-400 nm.

2. Instrument Description

The SBUV/2 instrument is a nadir-viewing Ebert-Fastie double monochromator that covers the wavelength range 160-406 nm with a 1.1 nm bandpass [*Frederick et al.*, 1986]. The primary purpose of the instrument is to measure stratospheric profile and total column ozone, using 12 discrete wavelengths between 252-340 nm during a 32 second scan. Solar irradiance measurements are made by deploying a diffuser plate when the polar-orbiting TIROS spacecraft crosses the day-night terminator. The instrument is required to accurately measure signals varying over more than six orders of magnitude. This is accomplished using three separate gain ranges, each with a gain of approximately 100 relative to the next range. Each gain range slightly overlaps the next, so that there are narrow regions of signal level where Range 1 and Range 2 (or Ranges 2 and 3) measurements are simultaneously valid. The fundamental quantity required for ozone determination is the directional albedo, defined as the ratio of radiance I_λ to irradiance F_λ. The only optical element not common to both radiance and irradiance measurements is the solar diffuser, so that careful monitoring of diffuser changes is critical to the creation of accurate ozone values. Each SBUV/2 instrument carries an onboard calibration system to track long-term changes in diffuser reflectivity [*Weiss et al.*, 1991]. Continuous scan (sweep mode) measure-

ments can also be performed, with samples taken at approximate 0.147 nm intervals over the full wavelength range. Each sweep scan takes 168 seconds, moving from long to short wavelengths, with an additional 24 seconds allotted for grating drive retrace and electronic calibration tests. NOAA-9 sweep solar measurements were normally performed for two consecutive scans on one orbit per day. A typical NOAA-9 SBUV/2 solar spectrum is shown in Figure 2.

2.1 Instrument Equation

Numerous correction terms are required to convert the observed instrument counts to solar irradiance values. These corrections include electronic offset, photomultiplier tube (PMT) temperature and gain dependence, response non-linearity, diffuser angular response (goniometry), diffuser reflectivity change, and prelaunch instrument responsivity. Extensive discussions for SBUV/2 instruments are given in *Hilsenrath et al.* [1995] and *Cebula et al.* [1998a]. We use the term "internally corrected solar data" to describe measurements which have been processed with these corrections, but no correction for long-term throughput change. Following *Cebula et al.* [1998a], the equation for internally corrected solar data can be written as:

$$C = (S - D)\, N\, T_{\mathrm{Corr}}\, G\, R\, A\, f_{\mathrm{Diff}} f_{\mathrm{AU}} \qquad [1]$$

$C(\lambda,t)$	internally corrected solar data [mW m^{-2} nm^{-1}]
$S(r,t)$	raw signal [counts]; r = gain range
$D(r,t)$	electronic offset [counts]
$N(r,S)$	nonlinearity correction
$T_{\mathrm{Corr}}(r,t)$	photomultiplier tube (PMT) temperature correction
$G(r,\lambda,t)$	interrange ratio
$R(\lambda)$	initial instrument responsivity [mW m^{-2} nm^{-1} $count^{-1}$]
$A(\lambda,\alpha,\beta)$	goniometric correction
$f_{\mathrm{Diff}}(\lambda,t)$	diffuser reflectivity correction
$f_{\mathrm{AU}}(t)$	solar distance correction (to 1 AU)

The hysteresis correction described by *DeLand et al.* [2001] is not required for solar irradiance data because these measurements are only taken at the end of the daylit portion of the orbit, where the hysteresis effect does not occur. Brief descriptions of each correction term are given below.

Electronic Offset $D(r,t)$: This quantity is introduced into the data stream to avoid counter underflow due to statistical fluctuations at low signal levels. Long-term variations in each gain range are tracked separately using night side data. Range 1 data were found to require a time-dependent correction, with a 1-2% effect on sweep solar data shortward of ~180 nm.

Non-linearity $N(r,S)$: Correction functions are derived from prelaunch laboratory measurements for all gain ranges. The typical magnitude of each correction is ~1-2%, and is a function of the observed PMT current (expressed as counts). The Range 3 non-linearity correction was recently revised using inflight ice reflectivity and sweep Earth data. The revised function does not change during the instrument lifetime, and improves the solar irradiance results at 260-300 nm, where low Range 3 data are observed.

PMT Temperature $T_{Corr}(r,t)$: The SBUV/2 radiometric sensitivity is temperature-dependent for gain range 1 and 2 data, which are measured from the PMT anode. The sensitivity is characterized prelaunch using the PMT temperature, and corrected for all inflight measurements based on concurrent instrument telemetry. The correction is approximately +2% for a typical NOAA-9 operating temperature of 10°C, with seasonal fluctuations of ±0.5%. These fluctuations increased to ±2% as NOAA-9 drifted through a near-terminator orbit, but no long-term drift was observed [*Ahmad et al.*, 1994].

Interrange Ratio $G(r,\lambda,t)$: Discrete mode measurements record data in all three gain ranges simultaneously, enabling in-orbit tracking of the gain ratios. Range 1 (the most sensitive) and Range 2 are both measured from the PMT anode, so that the gain between these ranges (IRR_{12}) is simply an electronic amplification factor. We expect IRR_{12} to be constant in wavelength and time, and this is confirmed by the results of *DeLand et al.* [2001]. Range 3 data are measured from the PMT cathode, so that the gain between these ranges (IRR_{23}) incorporates differences between the anode and cathode relationship. IRR_{23} is spectrally dependent, and both drifts and fluctuates over time. A full discussion of the procedure used to derive $IRR_{23}(t)$ is presented in *DeLand et al.* [2001].

Goniometric Correction $A(\lambda,\alpha,\beta)$: The solar diffuser plate response has an angular dependence, which is characterized as a function of spacecraft-centered elevation and azimuth angles. The elevation angle varies rapidly during each scan as the spacecraft passes the day-night terminator. The azimuth angle has a seasonal variation, and also experiences long-term changes as the nominal orbit drifts to later Equator-crossing times. Prelaunch measurements determined the goniometric response of the diffuser over a wide range of elevation and azimuth angles. Figure 3 shows that the NOAA-9 orbit drift led to azimuth angles outside the calibration range during large parts of 1989-1992. A revised goniometric correction was derived from inflight data using the method described in *Hilsenrath et al.* [1995]. However, some data were unusable because the diffuser was completely shadowed at $\beta < 11°$. A wavelength-dependent goniometric correction term is also required for data at $\lambda < 250$ nm to properly represent non-Lambertian effects.

Diffuser Reflectivity $f_{Diff}(\lambda,t)$: SBUV/2 instruments are designed with an onboard Hg lamp-based calibration system to track relative changes in diffuser reflectivity [*Weiss et al.*, 1991]. On NOAA-9, this system suffered from significant short-term instabilities, rendering the calibration data useless [*Frederick et al.*, 1986]. A period of increased frequency solar measurements was conducted in mid-1986 to provide a snapshot of diffuser reflectivity changes. Further information is given in Section 3.1.

2.2 Instrument Operations

NOAA-9 SBUV/2 was launched on December 30, 1984 and operated successfully from its initial Earth view measurements on February 10, 1985 until the sweep solar measurements were terminated on May 6, 1997. There are some gaps in the available solar data record due to occasional shadowing of the solar diffuser and spacecraft anomalies such as safe mode events. Table 1 lists all periods with data gaps greater than 10 days. Other instrument operations effects do not cause complete loss of irradiance data, but require correction in order to create the best product.

a. Diffuser Deployment. The NOAA-9 solar diffuser occasionally deployed to a position 0.25° less than its nominal deployment angle. This error leads to an irradiance increase of 0.8-1.3% at the high incidence angles used for SBUV/2 irradiance measurements (θ = 60-82°). Diffuser deployment errors do not trigger a flag in the instrument housekeeping data, and must be identified by inspection. These errors were corrected on a scan-by-scan basis in the final data set.

b. Goniometry at high azimuth angles. The NOAA-9 spacecraft experienced high spacecraft azimuth angles ($\beta > 57°$) during mid-1985, as shown in Figure 3. On many dates during this period, the solar irradiance data fluctuated by as much as 5-6% after applying the nominal goniometric correction, in a manner consistent with partial shadowing of the solar diffuser. While the elevation and azimuth angle values were within the prelaunch calibration range at this time, unforeseen effects can occur after an instrument is integrated onto the spacecraft. Correction functions for affected data have been derived using concurrent data from the SBUV/2 cloud cover radiometer (CCR) when viewing the Sun, which collects coincident data at 378.6 nm using a 1 second cadence. However, some azimuth angle-dependent errors are still present. The monochromator and CCR are approximately co-aligned, but do view slightly different regions of the solar diffuser plate. Similar but less frequent problems were observed during 1995-1997, when high azimuth angles appeared again.

c. Scan 1 measurement range. Due to problems with the software controlling the SBUV/2 grating drive, the first two major frames of data (361-406 nm) from the first scan of each NOAA-9 measurement sequence are unavailable. The prelaunch radiometric calibration is only valid to 400 nm, so that a typical NOAA-9 daily spectrum therefore represents only one sample in the wavelength range 361-400 nm rather than the normal two samples. This problem was corrected for all subsequent SBUV/2 instruments.

d. Grating drive sticking. Late in its lifetime, NOAA-9 began to experience occasional sticking of the grating drive. In sweep mode, this problem typically appeared at wavelengths shortward of 250 nm. The condition usually lasted only a few seconds, but in severe cases, all data shortward of the sticking point were lost until the grating drive retraced to its starting position. A listing of dates with complete data loss is provided with the final data set.

3. Time-Dependent Instrument Characterization

Numerous aspects of the NOAA-9 SBUV/2 instrument characterization changed during its lifetime, requiring derivation of corrections to the prelaunch calibration. The sweep mode grating drive performance changed in space, causing the nominal wavelength scale to drift by approximately –0.10 nm from 1985 to 1997. The change in wavelength scale was evaluated by fitting absorption lines in the observed solar spectrum to derive a nominal line center position. The absolute position may differ from reference values due to instrument resolution, but the time-dependent variation of these values indicates the instrument behavior. A similar procedure was used for SSBUV [*Cebula et al.*, 1996a], Nimbus-7 SBUV [*DeLand and Cebula*, 2001], and NOAA-11 SBUV/2 [*Cebula et al.*, 1998a]. Figure 4 shows an example of the data and fit for the Ca II K line at 393.4 nm. We derived a power law time dependence fit to these data, and applied the appropriate adjustment to the daily spectra. The accuracy of this correction is approximately

0.02 nm, which is comparable to the accuracy of the prelaunch wavelength calibration. *DeLand and Cebula* [2001] showed that the results of this method were consistent over the spectral range of Nimbus-7 SBUV.

3.1 Accelerated Diffuser Deployment

The NOAA-9 SBUV/2 onboard calibration system developed significant mercury lamp stability problems shortly after launch with intensity fluctuations of ±10% during a single sequence [*Frederick et al.*, 1986]. This problem prevented the use of the system to track diffuser reflectivity changes. In the absence of an onboard calibration system, a period of accelerated diffuser deployment was used to quantify instrument response changes due to diffuser degradation. During a 2-month period in summer 1986, sweep mode solar measurements were performed on every orbit (13-14 times per day). Figure 5 shows the accumulation of diffuser exposure time during the lifetime of NOAA-9 SBUV/2. If the diffuser reflectivity change is assumed to be proportional to diffuser exposure, then a multiple linear regression fit to irradiance around this period allows the separation of exposure-dependent and time-dependent response changes. This procedure was used four times for Nimbus-7 SBUV, and successfully characterized most response changes [*Schlesinger and Cebula*, 1992]. NOAA-9 SBUV/2 had only one accelerated deployment period early in its lifetime, and analysis of total ozone data indicates that the actual diffuser behavior began to diverge from predictions after 1992 [*Taylor et al.*, 2003]. *Schlesinger and Cebula* [1992] observed time-dependent changes in the Nimbus-7 diffuser exposure coefficients by virtue of having multiple accelerated deployment periods available. We have applied the accelerated deployment diffuser degradation correction to all NOAA-9 solar data in order to remove the downward step in irradiance associated with the summer 1986 measurements. This correction also reduces the magnitude of the remaining uncorrected instrument throughput change in the irradiance data. Any residual errors associated with changes in diffuser degradation coefficients during the later part of the NOAA-9 data record are removed by the SSBUV comparison analysis described in Section 3.3.

3.2 Solar Minimum Analysis

Determination of NOAA-9 SBUV/2 instrument throughput changes using internally corrected data requires the identification of reference irradiance values, either internal or external, for comparison. One approach is to take advantage of the low levels of solar activity during solar minimum conditions. The Mg II index core-to-wing ratio is a good indicator of solar UV activity on both solar rotational and solar cycle time scales [*Heath and Schlesinger*, 1986]. The rotational minimum values of the Nimbus-7 SBUV Mg II index varied by less than 0.5% during the 1985-1986 solar minimum period, as shown in Figure 6. This implies a very constant level of solar activity. The scale factors listed in *DeLand and Cebula* [1993] can be used with the Nimbus-7 Mg II index to model the irradiance variations associated with small Mg II index changes between successive rotational minima. Twenty-two (22) rotational minima during this period were selected for analysis. After applying the diffuser degradation correction from Section 3.1 and the Mg II index prediction, we assumed that the remaining time-dependent variation during 1985-1986 represents instrument throughput change. The derived response changes are approximately linear with time, varying from –8% at 200 nm to < 1% longward of 370 nm. The same method was used to constrain NOAA-9 response changes after the last SSBUV flight in

January 1996 (see Section 3.3). Ten solar rotation minima were selected during the period August 1996 – May 1997 to apply this method. For this short period, derived instrument response changes do not show a clear time dependence. The magnitude of the instrument response changes is consistent with the SSBUV-8 coincident ratio results from January 1996 (see Section 3.3).

3.3 SSBUV Comparisons

The engineering model of the SBUV/2 instrument was reconfigured to operate on the Space Shuttle, and flew eight missions between 1989 and 1996. The purpose of these SSBUV flights was to provide intercomparison and calibration reference data for on-orbit SBUV/2 instruments [*Hilsenrath et al.*, 1988]. Extensive radiometric calibrations were performed before, during, and after each mission, providing accurate corrections for all measurements. A description of the use of SSBUV ozone data for correction of SBUV/2 ozone products is given by *Hilsenrath et al.* [1995]. Comparisons of flight-averaged SSBUV solar spectra show flight-to-flight agreement within 1% [*Cebula et al.*, 1998b]. We have used coincident NOAA-9 and SSBUV solar measurements to evaluate NOAA-9 throughput changes during 1989-1996, following the procedure of *Cebula et al.* [1998a] that was developed for NOAA-11 SBUV/2. Full details of the method are discussed in *Cebula et al.* [1998a], and only a brief summary is given here. The absolute calibration difference between NOAA-9 and SSBUV was determined using initial NOAA-9 data from March 1985 (Figure 7). The magnitude and spectral dependence of this difference are comparable to the NOAA-11 calibration difference shown in *Cebula et al.* [1998a]. The SSBUV solar irradiance data agree with other coincident irradiance measurements to ±2% or better, as demonstrated in *Cebula et al.* [1996b] and *Woods et al.* [1996]. Therefore, we assume that the majority of the variation in Figure 7 represents NOAA-9 absolute calibration errors. The structure at the Mg II and Ca II absorption features indicates localized wavelength scale differences at the 0.02 nm level. The peak at 232 nm is caused by a Wood's anomaly in the NOAA-9 SBUV/2 grating [*Fowler*, 1993]. Using temporally coincident NOAA-9 and SSBUV data at later dates removes possible errors due to solar activity variations between dates. The SSBUV data were normalized to Flight #8 irradiance values at 400 nm. This adjustment was typically ±0.5% or less. SSBUV-1 data between 210-270 nm were increased by 1-2% for consistency with SSBUV-2 and SSBUV-3, which had the same level of solar activity. Exact NOAA-9 coincidence data were not available for the SSBUV-1 (October 1989) and SSBUV-2 (October 1990) flights due to NOAA-9 shadowing problems. We replaced these data with NOAA-9 measurements from approximately 27 days before SSBUV-1 and 54 days after the SSBUV-2 flight date to minimize differences in solar activity. The Mg II index change between the SSBUV flight dates and the selected NOAA-9 dates was 1%. We calculated an irradiance correction using the scale factors to adjust the NOAA-9 data to the SSBUV date. The uncertainty in this adjustment is 0.1% for wavelengths longward of 210 nm. The ratio of coincident NOAA-9 and SSBUV spectra, normalized by the initial calibration difference, then gives the relative NOAA-9 response for the date of each Shuttle flight.

Figure 8 shows the spectral dependence of these values for three selected SSBUV flights. The SSBUV radiometric calibration only covers the wavelength range 200-406 nm. Therefore, another technique is required to derive a sensitivity correction for the NOAA-9 data in the 170-200 nm region. We have chosen to use time series of NOAA-9 irradiance data at 5 nm intervals be-

tween 170-210 nm, with solar activity estimated by the Mg II index and scale factors and removed, to represent the instrument response change. This technique was also used by *Cebula et al.* [1998*a*] to derive sensitivity corrections at 170-200 nm for the NOAA-11 SBUV/2 data. *Cebula et al.* [1998*a*] note that this approach makes the assumption that the Mg II-based prediction is reasonably close to the actual long-term solar variation. The close agreement between the 200-210 nm time series values shown in Figure 8 and the SSBUV ratio values for the same dates support this assumption. Although the method described here is somewhat circular, we feel that it provides the best available correction for the NOAA-9 short wavelength data. Users are nevertheless cautioned as to the possible limitations of the results for determining long-term solar variations between 170-200 nm. NOAA-9 irradiance data shortward of 170 nm were found to be too noisy for effective use. Finally, smoothing spline fits (CLOESS) based on loess fitting methods described by *Cleveland and Grosse* [1991] are used to create a smooth representation of the spectrally dependent NOAA-9 response change corresponding to each SSBUV flight.

3.4 Corrected Irradiance Data

The final NOAA-9 SBUV/2 instrument response change function was determined by calculating 5 nm band average time series from the irradiance ratios of Sections 3.2 and 3.3, then fitting each time series with the CLOESS spline function. The density of points for each solar minimum period was reduced to avoid introducing unnecessary structure in the spline fits. Figure 9 shows examples of these combined results for four selected wavelength bands. Overall throughput corrections range from 22% at 200-205 nm to 2% at 395-400 nm. These spline functions then provide a basis to calculate daily instrument response changes, which are interpolated across the SBUV/2 wavelength range to create a spectrally dependent instrument response function corresponding to the date of each measured solar spectrum. The NOAA-9 internally corrected spectral irradiance data were processed using instrument corrections developed with this procedure.

4. Irradiance Results

The corrected NOAA-9 SBUV/2 irradiance data were binned to 1 nm intervals for consistency with other publicly available UV irradiance data sets. Figure 10 shows the time series of these data averaged between 200-205 nm. The solar cycle variation in panel (a) is approximately 9.3% from solar minimum in 1986 to the maximum 81-day averaged values in late 1989 and early 1992. Rotational modulation variations reached approximately 6% peak-to-peak during solar maximum. The NOAA-9 result is consistent with the Nimbus-7 SBUV estimate of 8.3(±2.6)% for Cycle 21 [*DeLand and Cebula*, 2001]. UARS SUSIM observed a range of ~10% at 208 nm for daily values during Cycle 22 [*Floyd et al.*, 2002], while UARS SOLSTICE determined an averaged solar cycle variation of 6(±2)% [*Rottman et al.*, 2001]. The lower panel of Figure 10 shows the difference between the NOAA-9 irradiance data and solar variations predicted by the Mg II index and scale factor model. The long-term agreement is generally within ±1%, consistent with the results obtained by *DeLand and Cebula* [1998b] for NOAA-11 SBUV/2. Larger differences observed for short time periods during 1990-1992 probably reflect problems with the NOAA-9 calibration in near-terminator orbit conditions. Figure 11(a) shows NOAA-9 data averaged over 245-250 nm. The observed solar cycle variation is approximately 5.7%. This is consistent with the Nimbus-7 SBUV estimate of 4.9(±1.8)% at 240-245 nm for Cycle 21. Differences from the Mg II index prediction are ±1% or less. Figure 12(a) shows NOAA-9 data av-

eraged over 305-310 nm. Variations in these data are ±1% or less. Since solar variability in this wavelength range is expected to be significantly less that 1%, this provides an indication of the accuracy of the NOAA-9 sensitivity correction.

4.1. Uncertainty Analysis

Cebula et al. [1998a] present extensive discussion of absolute and time-dependent uncertainty analysis for NOAA-11 SBUV/2 irradiance data. Since the absolute calibration procedures are very similar between SBUV/2 instruments, we do not repeat that description here. We followed the same approach. Table 2 summarizes terms contributing to the time-dependent instrument characterization. As noted in Section 3.1, errors in the accuracy of the diffuser reflectivity correction are removed by the instrument sensitivity analysis. We adopt 0.2% (2σ) for the uncertainty in this term, following *Cebula et al.* [1998a]. The uncertainty estimate for the time-dependent interrange ratio is 0.5% (2σ). The instrument sensitivity correction uncertainty value reflects the choice of CLOESS spline fit tension, because it is difficult to ascertain whether variations at the 0.5-1.0% level are true sensitivity changes or instrument noise. The wavelength scale correction, SSBUV, and short wavelength ($\lambda < 200$ nm) uncertainty values are taken from *Cebula et al.* [1998a]. Combining these terms gives an RSS error estimate of ±1.2% (2σ) for NOAA-9 irradiance data variations at long wavelengths, increasing to ±2.3% for solar cycle variations at 205 nm. Larger uncertainties are appropriate in late 1990 and early 1991, where the goniometric correction is difficult due to the near-terminator orbit.

4.2. Solar Cycle Variability

Willson and Mordvinov [1993] have proposed a secular trend in total solar irradiance (TSI) of approximately +0.03%/decade, based on differences between solar minimum TSI values. *Lean et al.* [1997] suggest that integrated solar UV variations between 200-400 nm represent up to 30% of TSI variations. Thus, we can examine the NOAA-9 SBUV/2 data for UV irradiance variations between solar minima. Approximate dates for the lowest solar activity levels during the solar cycle 21 and 22 minima observed by NOAA-9 are September 1986 and September 1996, respectively [*Harvey and White*, 1999]. We created spectra for each period to evaluate possible spectral irradiance changes, averaging three days to reduce noise. The difference between Cycle 22 and Cycle 21 minimum irradiance values is shown in Figure 13. The magnitude is generally ±1% or less. Given the magnitude of the uncertainties listed in Table 2, these irradiance differences should not be considered statistically significant. For comparison, the spectral dependence of the cycle 22 variation from maximum in June 1989 to minimum in September 1986 is shown in Figure 14. This variation is consistent with the peak-to-peak irradiance variation for cycle 22 shown by *Floyd et al.* [2002]. The dotted line in Figure 14 shows the predicted irradiance variation between the same dates calculated using NOAA SEC Mg II index values and 1 nm averaged scale factors. The agreement is within 1%, except for lower observed irradiance variations at the peak of the Mg II and Mg I lines. This result supports the idea that the scale factors, which are derived from short-term irradiance variations, can be successfully used to estimate long-term irradiance variations in the middle ultraviolet.

5. Intercomparisons

The timeline in Figure 1 shows that there are many opportunities for intercomparison of NOAA-9 SBUV/2 irradiance data with other satellite instruments. A complete analysis over all wavelengths will be presented at a later date. In this paper, we present comparisons using data averaged between 200-205 nm as an illustration because of its significance for stratospheric photochemistry. Figure 15 shows absolute irradiance time series of 200-205 nm data from all published data sets. An initial conclusion from this figure is that, while absolute calibration differences of 5-10% (larger for Nimbus-7 SBUV) exist between different instruments, all data sets reproduce the basic features of observed solar variability (rotational modulation, 11-year cycle). Figure 16 shows time series of the difference between the NOAA-9 200-205 nm data and each overlapping data set. For each panel, the average bias has been removed to facilitate examination of time-dependent differences. There are no long-term drifts larger than 2% between NOAA-9 SBUV/2 and other satellite instruments. Short-term fluctuations in Figure 16(a) are largely due to periodic variations in Nimbus-7 SBUV data [*DeLand and Cebula*, 2001]. Other recent multi-satellite irradiance comparisons include *DeLand and Cebula* [1998b] (NOAA-11, SUSIM, UARS SOLSTICE), *DeLand and Cebula* [2001] (Nimbus-7, SME), and *DeLand et al.* [2003] (UARS SUSIM, UARS SOLSTICE). Taken together, these comparisons provide a realistic estimate of the present long-term uncertainty in solar UV irradiance data sets. An important next step is the creation of a unified spectral irradiance data set covering the period 1978-2002, which requires additional judgments as to which data set to use during intervals with multiple working instruments. Such an analysis is beyond the scope of this paper.

6. Conclusion

We have developed a long-term instrument characterization for NOAA-9 SBUV/2 solar spectral UV irradiance data, using coincidences with Shuttle SBUV measurements to quantify NOAA-9 temporal changes. The corrected NOAA-9 data provide daily spectra between 170-400 nm from March 1985 to May 1997, covering the full range of solar cycle 22. Solar cycle amplitudes determined from these data are consistent with previous results for cycles 21 and 22. The complete NOAA-9 irradiance data set is available at http://ozone.sesda.com/solar/, and will be archived at the National Geophysical Data Center (NGDC). In the near future, we hope to combine these data with other measurements to produce a unified spectral irradiance data set covering 25 years from 1978 to the present.

Acknowledgements

This work was supported by NASA grant NAS1-98106. The raw SBUV/2 data were obtained from NOAA/NESDIS with support from the NOAA Climate and Global Change Atmospheric Chemistry Element.

References

Ahmad, Z., M. T. DeLand, R. P. Cebula, H. Weiss, C. G. Wellemeyer, W. G. Planet, J. H. Lienesch, H. D. Bowman, A. J. Miller, and R. M. Nagatani, Accuracy of total ozone retrieval from NOAA SBUV/2 measurements: Impact of instrument performance, *J. Geophys. Res.*, *99*, 22,975-22.984, 1994.

Arnold, N. F., and T. R. Robinson, Solar cycle changes to planetary wave propagation and their influence on the middle atmosphere circulation, *Ann. Geophysicae*, *16*, 69-76, 1998.

Balachandran, N. K., D. Rind, P. Lonergan, and D. T. Shindell, Effects of solar cycle variability on the lower stratosphere and the troposphere, *J. Geophys. Res.*, *104*, 27,321-27,339, 1999.

Callis, L. B., M. Natarajan, and J. D. Lambeth, Calculated upper stratospheric effects of solar UV flux and NO_y variations during the 11-year solar cycle, *Geophys. Res. Lett.*, *27*, 3869-3872, 2000.

Canty, T., and K. Minschwaner, Seasonal and solar cycle variability of OH in the middle atmosphere, *J. Geophys. Res.*, *107*(D24), 4737, doi:10.1029/2002JD002278, 2002.

Cebula, R. P., E. Hilsenrath, P. W. DeCamp, K. Laamann, S. Janz, and K. McCullough, The SSBUV experiment wavelength scale and stability: 1988 to 1994, *Metrologia*, *32*, 633-636, 1996.

Cebula, R. P., G. O. Thullier, M. E. VanHoosier, E. Hilsenrath, M. Herse, G. E. Brueckner, and P. C. Simon, Observations of the solar irradiance in the 200-350 nm interval during the ATLAS-1 mission: A comparison among three sets of measurements-SSBUV, SOLSPEC, and SUSIM, *Geophys. Res. Lett.*, *23*, 2289-2292, 1996b.

Cebula, R. P., M. T. DeLand, and E. Hilsenrath, NOAA 11 Solar Backscattered Ultraviolet, model 2 (SBUV/2) instrument solar spectral irradiance measurements in 1989-1994, 1. Observations and long-term calibration, *J. Geophys. Res.*, *103*, 16,235-16,249, 1998a.

Cebula, R. P., L.-K. Huang, and E. Hilsenrath, SSBUV sensitivity drift determined using solar spectral irradiance measurements, *Metrologia*, *35*, 677-683, 1998b.

Chandra, S., J. R. Ziemke, and R. W. Stewart, An 11-year solar cycle in tropospheric ozone from TOMS measurements, *Geophys. Res. Lett.*, *26*, 185-188, 1999.

Cleveland, W. S., and E. Grosse, Computational methods for local regression, *Stat. And Comput.*, *1*, 47-62, 1991.

DeLand, M. T., and R. P. Cebula, Composite Mg II solar activity index for solar cycles 21 and 22, *J. Geophys. Res.*, *98*, 12,809-12,823, 1993.

DeLand, M. T., and R. P. Cebula, Solar UV activity at solar cycle 21 and 22 minimum from NOAA-9 SBUV/2 data, *Sol. Phys.*, *177*, 105-116, 1998a.

DeLand, M. T., and R. P. Cebula, NOAA 11 Solar Backscattered Ultraviolet, model 2 (SBUV/2) instrument solar spectral irradiance measurements in 1989-1994, 2. Results, validation, and comparisons, *J. Geophys. Res.*, *103*, 16,251-16,273, 1998b.

DeLand, M. T., and R. P. Cebula, Spectral solar UV irradiance data for cycle 21, *J. Geophys. Res.*, *106*, 21,569-21,583, 2001.

DeLand, M. T., R. P. Cebula, L.-K. Huang, S. L. Taylor, R. S. Stolarski, and R. D. McPeters, Observations of "hysteresis" in backscattered ultraviolet ozone data, *J. Atmos. Ocean Tech.*, *19*, 914-924, 2001.

DeLand, M. T., L. E. Floyd, G. J. Rottman, and J. M. Pap, Status of UARS solar UV irradiance data, *Adv. Space Res.*, in press, 2003.

Floyd, L. E., D. K. Prinz, P. C. Crane, and L. C. Herring, Solar UV irradiance variation during cycles 22 and 23, *Adv. Space Res.*, *29*, 1957-1962, 2002.

Fowler, W. F., Wood's anomalies in the SBUV/2, Ball Aerospace System Engineering Report **SBUV-WF-93-721**, 5 pp., December 1993.

Frederick, J. E., R. P. Cebula, and D. F. Heath, Instrument characterization for the detection of long-term changes in stratospheric ozone: An analysis of the SBUV/2 radiometer, *J. Atmos. Ocean Tech.*, *3*, 472-480, 1986.

Haigh, J. D., Modelling the impact of solar variability on climate, *J. Atmo. Solar-Terr. Phys.*, *61*, 63-72, 1999.

Harvey, K. L., and O. R. White, What is solar cycle minimum?, *J. Geophys. Res.*, *104*, 19,759-19,764, 1999.

Heath, D. F., Observations of the intensity and variability of the near ultraviolet solar flux from the Nimbus 3 satellite, *J. Atmo. Sci.*, *26*, 1157-1160, 1969.

Heath, D. F., and B. M. Schlesinger, The Mg-280 nm doublet as a monitor of changes in solar ultraviolet irradiance, *J. Geophys. Res.*, *91*, 8672-8682, 1986.

Heath, D. F., and M. P. Thekaekara, The solar spectrum between 1200 and 3000 Å, in *The Solar Output and Its Variation*, ed. O. R. White, pp. 193-212, Colo. Assoc. of Univ. Press, Boulder, Colorado, 1977.

Hilsenrath, E., D. Williams, and J. Frederick, Calibration of long term data sets from operational satellites using the Space Shuttle, *SPIE Proc.*, *924*, 215-222, 1988.

Hilsenrath, E., R. P. Cebula, M. T. DeLand, K. Laamann, S. Taylor, C. Wellemeyer, and P. K. Bhartia, Calibration of the NOAA 11 solar backscatter ultraviolet (SBUV/2) ozone data set from 1989 to 1993 using in-flight calibration data and SSBUV, *J. Geophys. Res.*, *100*, 1351-1366, 1995.

Hood, L. L., Effects of short-term solar UV variability on the stratosphere, *J. Atmo. Solar-Terr. Phys.*, *61*, 45-51, 1999.

Hood, L. L., and S. Zhou, Stratospheric effects of 27-day solar ultraviolet variations: The column ozone response and comparisons of solar cycles 21 and 22, *J. Geophys. Res.*, *104*, 26,473-26,479, 1999.

Khosravi, R., G. Brasseur, A. Smith, D. Rusch, S. Walters, S. Chabrillat, and G. Kockarts, Response of the mesosphere to human-induced perturbations and solar variability calculated by a 2-D model, *J. Geophys. Res.*, *107*(D18), 4358, doi:10.1029/2001JD001235, 2002.

Kodera, K., and Y. Kuroda, Dynamical response to the solar cycle, *J. Geophys. Res.*, *107*(D24), 4749, doi:10.1029/2002JD002224, 2002.

Lean, J. L., G. J. Rottman, H. L. Kyle, T. N. Woods, J. R. Hickey, and L. C. Puga, Detection and parameterization of variations in solar mid- and near-ultraviolet radiation (200-400 nm), *J. Geophys. Res.*, *102*, 29,939-29,956, 1997.

Lee, H., and A. K. Smith, Simulation of the combined effects of solar cycle, quasi-biennal oscillation, and volcanic forcing on stratospheric ozone changes in recent decades, *J. Geophys. Res.*, *108*(D2), 4049, doi:10.1029/2001JD001503, 2003.

Meier, R. R., Ultraviolet spectroscopy and remote sensing of the upper atmosphere, *Space Sci. Rev.*, *58*, 1-185, 1991.

Prag, A. B., and F. A. Morse, Variations in the solar ultraviolet flux from July 13 to August 9, 1968, *J. Geophys. Res.*, *75*, 4613-4621, 1970.

Rottman, G. J., Observations of solar UV and EUV variability, *Adv. Space Res.*, *8*(7), 53-66, 1988.

Rottman, G., T. Woods, M. Snow, and G. DeToma, The solar cycle variation in ultraviolet irradiance, *Adv. Space Res.*, *27*, 1927-1932, 2001.

Schlesinger, B. M., and R. P. Cebula, Solar variation 1979-1987 estimated from an empirical model for changes with time in the sensitivity of the Solar Backscatter Ultraviolet instrument, *J. Geophys. Res.*, *97*, 10,119-10,134, 1992.

Shindell, D., D. Rind, N. Balachandran, J. Lean, and P. Lonergan, Solar cycle variability, ozone and climate, *Science*, *284*, 305-308, 1999.

Smith, E. V. P., and D. M. Gottlieb, Solar flux and its variations, *Space Sci. Rev.*, *16*, 771-802, 1974.

Taylor, S. L., R. P. Cebula, M. T. DeLand, L.-K. Huang, R. S. Stolarski, and R. D. McPeters, Improved calibration of NOAA-9 and NOAA-11 SBUV/2 total ozone data using in-flight validation methods, *Int. J. Remote Sensing*, *24*, 315-328, 2003.

Van Loon, H., and D. J. Shea, The global 11-year solar signal in July-August, *Geophys. Res. Lett.*, *27*, 2965-2968, 2000.

Viereck, R., and L. C. Puga, The NOAA Mg II core-to-wing solar index: Construction of a 20-year time series of chromospheric variability from multiple satellites, *J. Geophys. Res.*, *104*, 9995-10,005, 1999.

Weiss, H., R. P. Cebula, K. Laamann, and R. D. Hudson, Evaluation of the NOAA 11 Solar Backscatter Ultraviolet radiometer, mod 2 (SBUV/2): Inflight calibration, *Proc. SPIE Int. Soc. Opt. Eng.*, *1493*, 80-90, 1991.

Willson, R. C., and A. V. Mordvinov, Secular total solar irradiance trend during solar cycles 21-23, *Geophys. Res. Lett.*, *30*(5), 1199, doi:10.1029/2002GL016038, 2003.

Woods, T. N., et al., Validation of the UARS solar ultraviolet irradiances: Comparisons with the ATLAS 1 and 2 measurements, *J. Geophys. Res.*, *101*, 9541-9569, 1996.

Zhou, S., A. J. Miller, and L. L. Hood, A partial correlation analysis of the stratospheric ozone response to 27-day solar UV variations with temperature effect removed, *J. Geophys. Res.*, *105*, 4491-4500, 2000.

TABLE 1
NOAA-9 SBUV/2 Solar Data Gaps (10 days or more)

Missing Data Period	Comment
13 Sep 1988 – 13 Nov 1988	solar array shadowing
19 Sep 1990 – 22 Nov 1990	shadowing (low azimuth)
21 Jan 1991 – 28 Feb 1991	shadowing (low azimuth)
1 Mar 1991 – 31 Mar 1991	no data (file lost)
1 Aug 1993 – 31 Aug 1993	no data (instrument shut down, NOAA-13 launch)
1 Aug 1995 – 15 Sep 1995	no data (safe mode/restart)
22 May 1996 – 18 Jun 1996	no data (ground processing software)

TABLE 2
NOAA-9 SBUV/2 Time-dependent Uncertainty Budget

Correction Term	180 nm	205 nm	250 nm	350 nm
Thermal sensitivity	0.2	0.2	0.2	—
Diffuser reflectivity	0.2	0.2	0.2	0.2
Interrange ratio IRR_{23}	0.5	0.5	0.5	—
Instrument sensitivity fits	2.0	2.0	1.5	1.0
Wavelength scale correction	0.2	0.3	0.1	0.1
SSBUV repeatability	—	0.9	0.6	0.4
SSBUV normalization	—	0.5	0.5	0.5
Short wavelength characterization	2.0	—	—	—
RSS total, %	2.9	2.3	1.8	1.2

All uncertainties are $\pm 2\sigma$ in percent.

Figure Captions

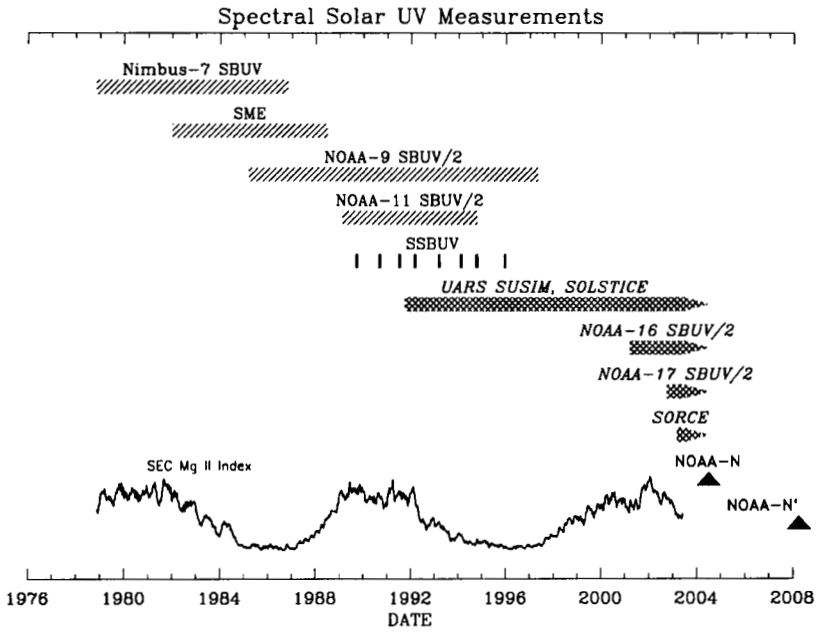

Figure 1. Timeline of satellite solar UV measurements since 1978. The 27-day averaged time series of the NOAA SEC Mg II index time series [*Viereck and Puga*, 1999] is shown for reference.

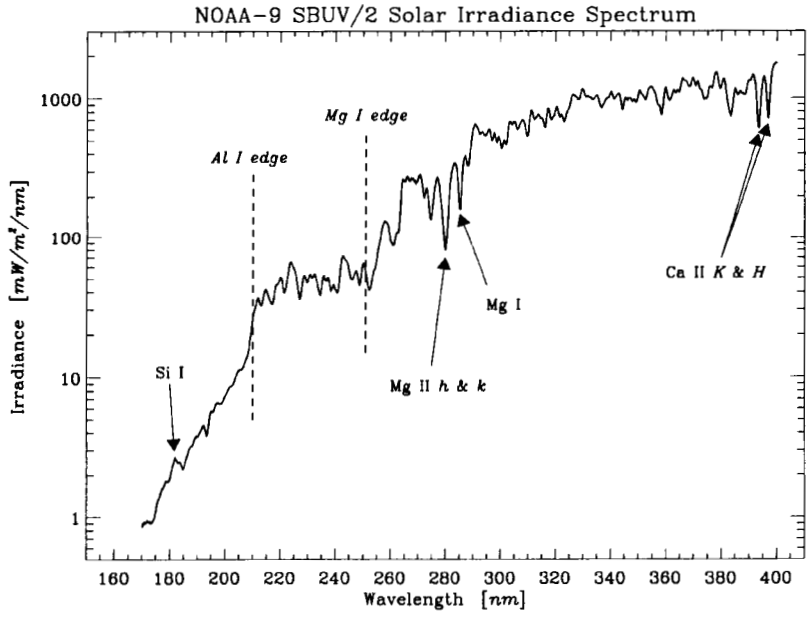

Figure 2. Typical NOAA-9 SBUV/2 solar irradiance spectrum, with significant features identified.

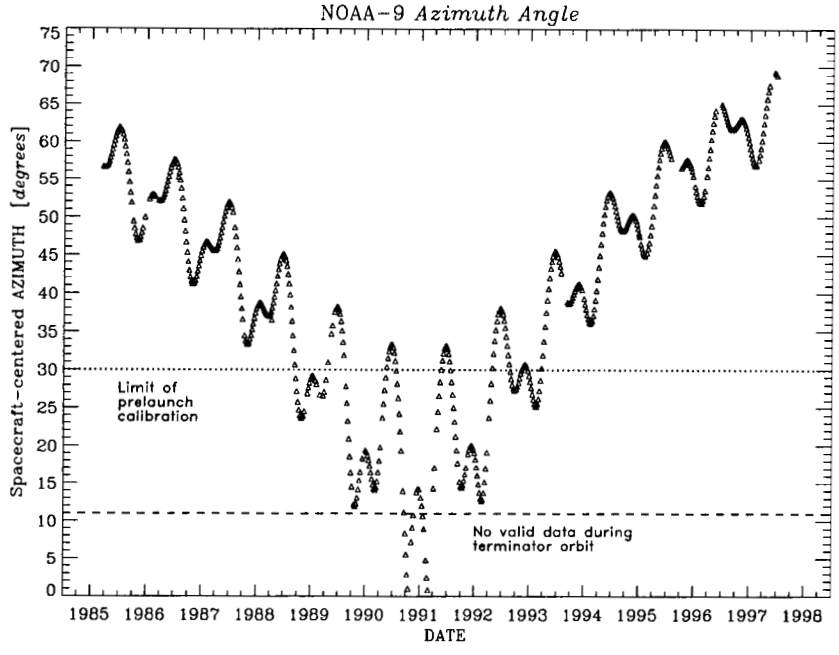

Figure 3. Time series of NOAA-9 spacecraft-centered azimuth angle.

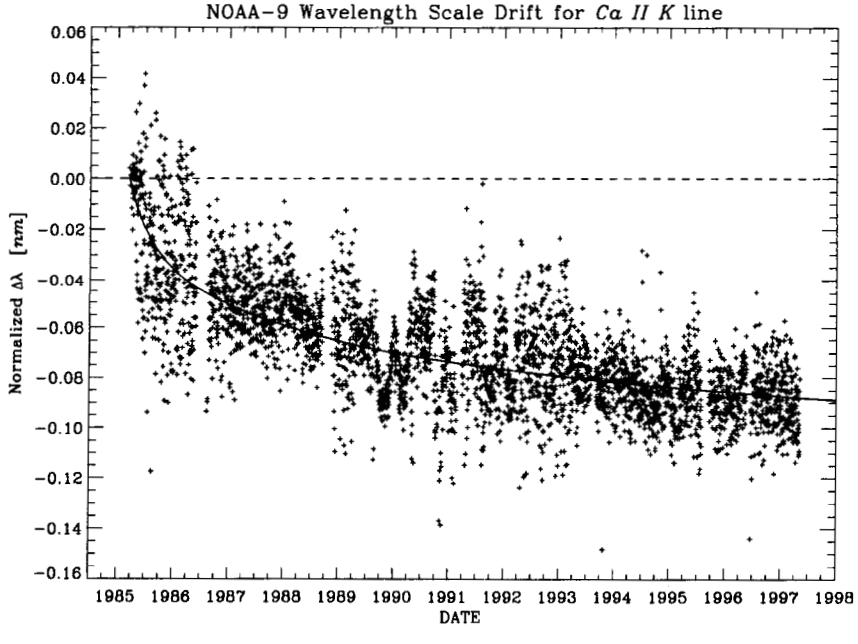

Figure 4. NOAA-9 SBUV/2 relative sweep mode wavelength scale drift, derived from measurements of the Ca II K absorption line at 393.4 nm. The solid curve is a power law fit to the data.

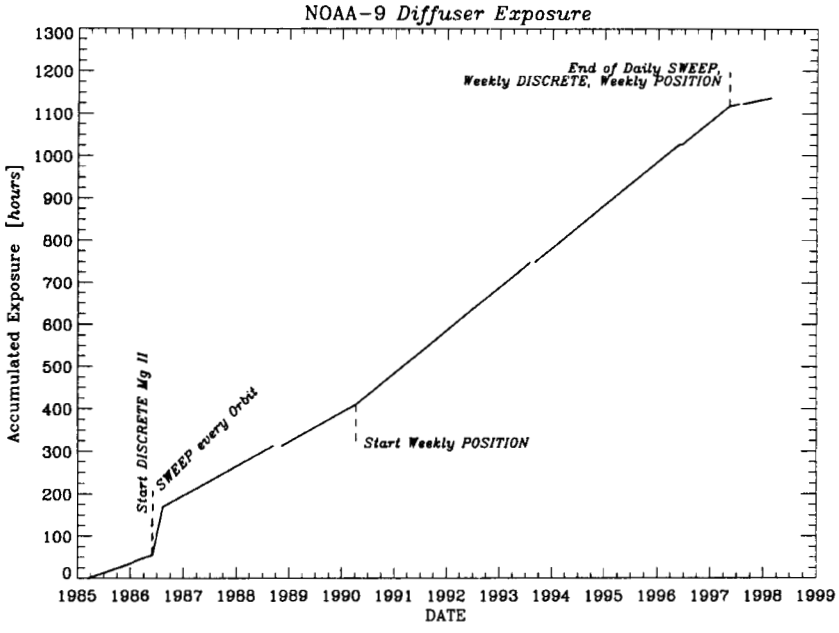

Figure 5. NOAA-9 SBUV/2 cumulative solar diffuser exposure time *vs.* calendar date. The rapid increase in mid-1986 represents the period of accelerated diffuser deployment discussed in Section 3.1. Other slope changes correspond to less significant changes in operational frequency.

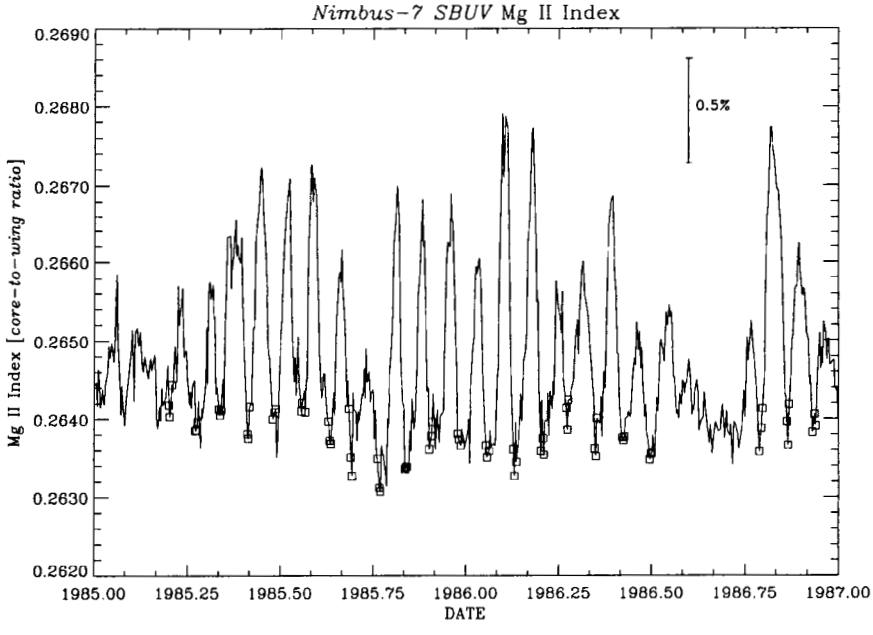

Figure 6. Nimbus-7 SBUV Mg II index values for 1985-1986. Squares indicate dates used for NOAA-9 SBUV/2 sensitivity change analysis.

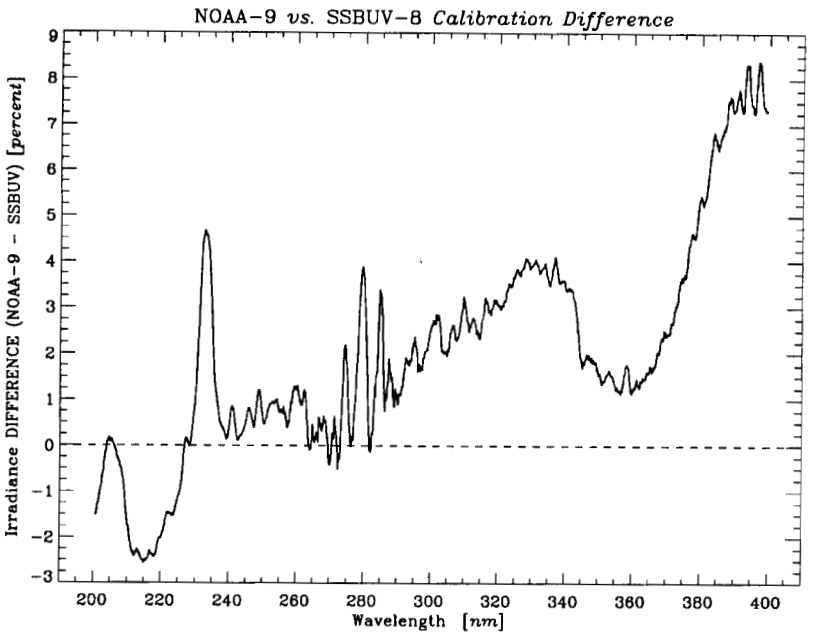

Figure 7. Difference between NOAA-9 initial on-orbit sweep solar measurements (March 1985) and flight-averaged solar data from SSBUV-8 (January 1996). Adjusted for difference in solar activity using Mg II index and scale factors.

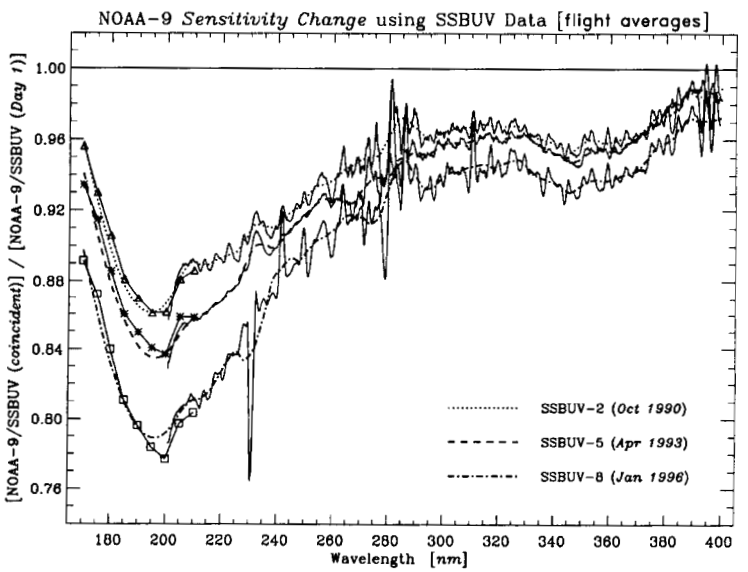

Figure 8. Ratio between NOAA-9 SBUV/2 and SSBUV flight-averaged solar spectra for dates of three SSBUV flights: #2 (October 1990), #5 (April 1993), #8 (January 1996). All ratios have been corrected for initial absolute calibration differences using results from Figure 7. The symbols plotted between 170-210 nm represent sensitivity change at each date estimated from time series data, as discussed in the text.

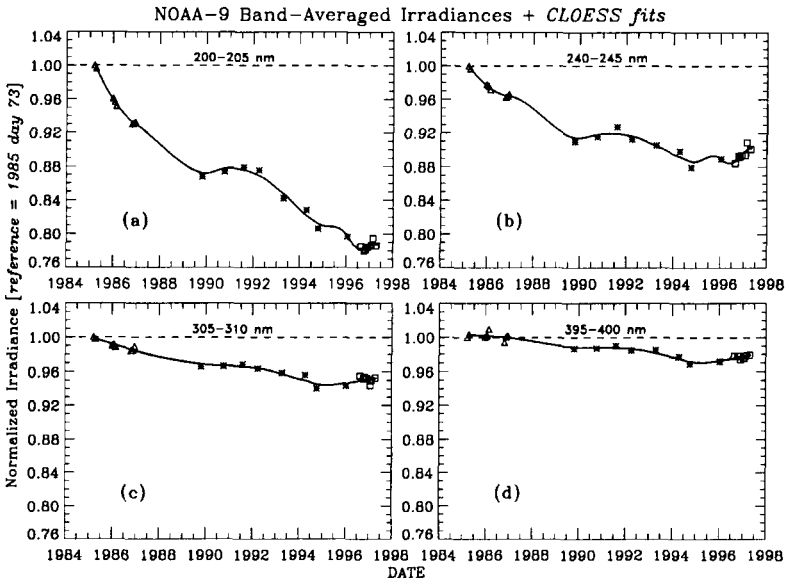

Figure 9. (a) Time series of NOAA-9 internally corrected data averaged between 200-205 nm, normalized to the start of measurements. *Triangles* = averages during 1985-1986 solar minimum, *squares* = averages during 1996-1997 solar minimum, *asterisks* = SSBUV ratios, *solid line* = CLOESS fit to data. (b) Time series of NOAA-9 normalized internally corrected data averaged between 240-245 nm. Symbols are same as in panel a. (c) Time series of NOAA-9 normalized internally corrected data averaged between 305-310 nm. (d) Time series of NOAA-9 normalized internally corrected data averaged between 395-400 nm.

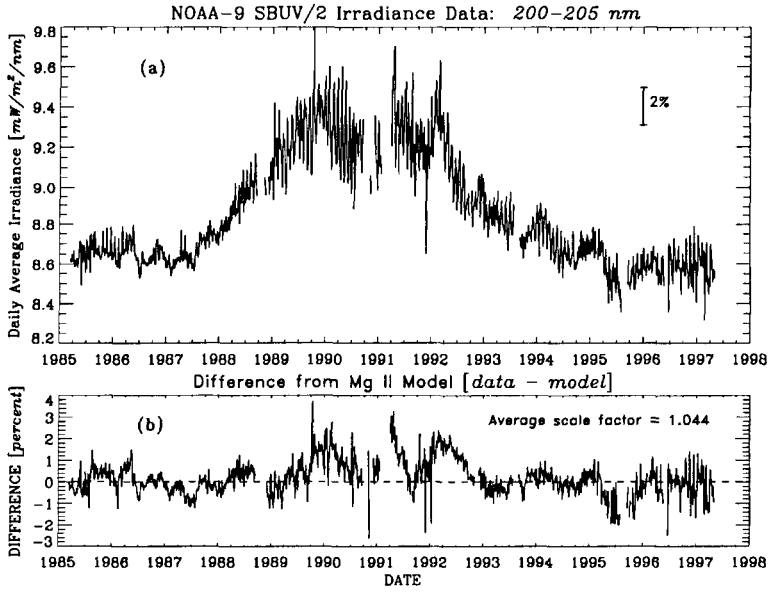

Figure 10. (a) Time series of NOAA-9 SBUV/2 calibrated irradiance data averaged between 200-205 nm. A 5-point binomial-weighted average has been applied to the data. (b) Difference between NOAA-9 200-205 nm data and variation predicted by Mg II index and scale factors, normalized to start of data set. A 5-point running average has been applied to the residual data.

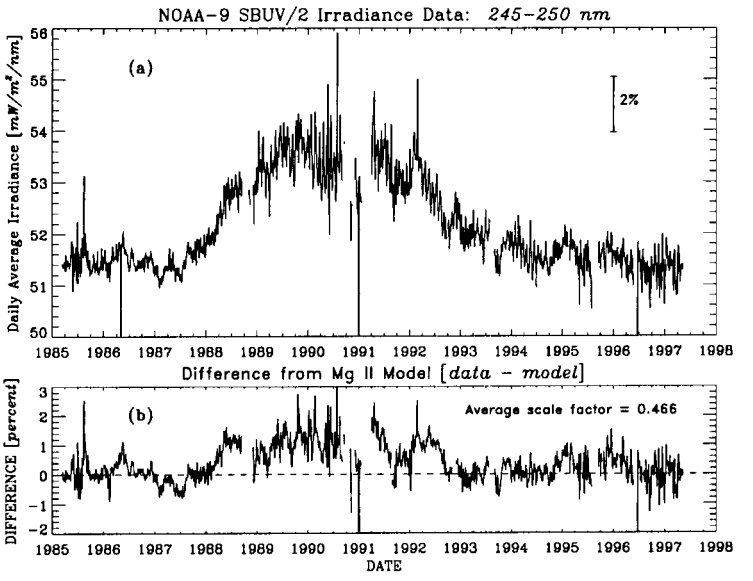

Figure 11. (a) Time series of NOAA-9 SBUV/2 calibrated irradiance data averaged between 245-250 nm. A 5-point binomial-weighted average has been applied to the data. (b) Difference between NOAA-9 245-255 nm data and variation predicted by Mg II index and scale factors, normalized to start of data set. A 5-point running average has been applied to the residual data.

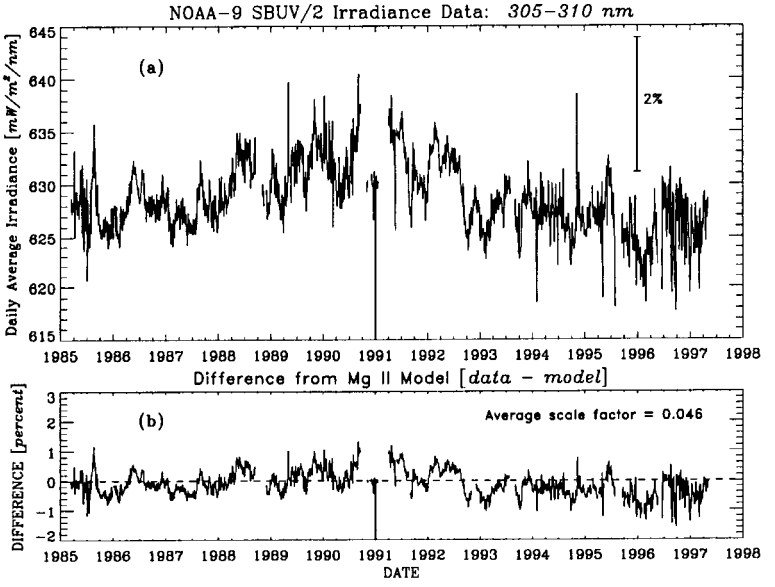

Figure 12. (a) Time series of NOAA-9 SBUV/2 calibrated irradiance data averaged between 305-310 nm. A 5-point binomial-weighted average has been applied to the data. (b) Difference between NOAA-9 305-310 nm data and variation predicted by Mg II index and scale factors, normalized to start of data set. A 5-point running average has been applied to the residual data.

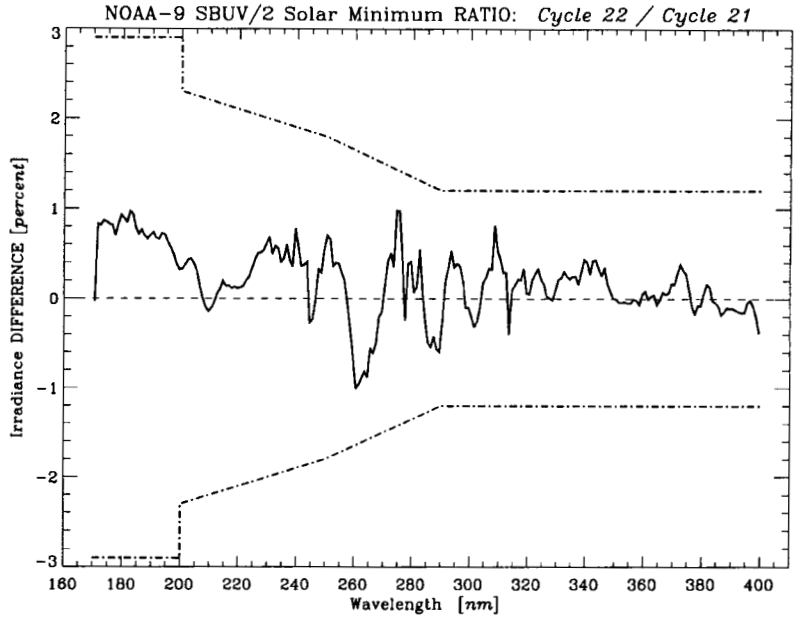

Figure 13. Change in NOAA-9 SBUV/2 spectral irradiance from the minimum of solar cycle 21 to the minimum of solar cycle 22. A 5-pt running average has been applied. *Dot-dashed line* = $\pm 2\sigma$ uncertainty in long-term instrument characterization.

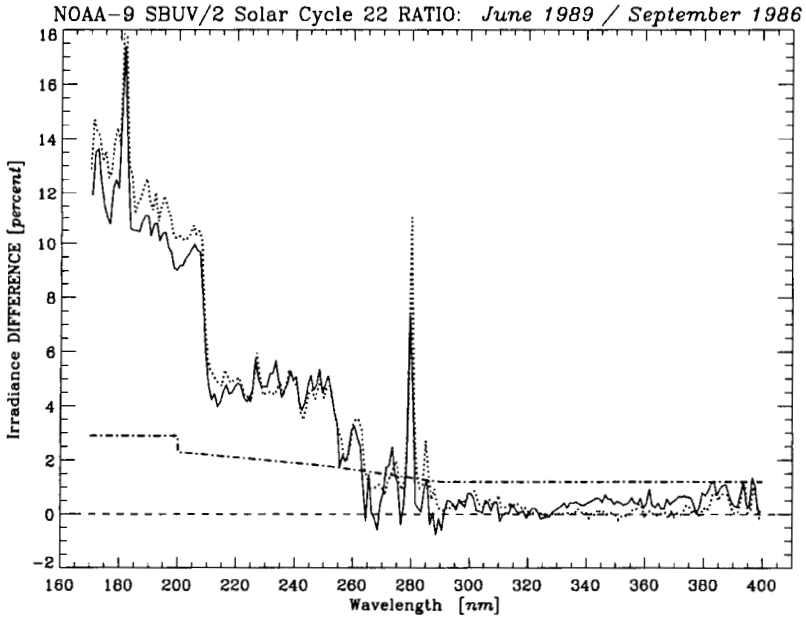

Figure 14. Change in NOAA-9 SBUV/2 spectral irradiance from the maximum to the minimum of solar cycle 22. *Dot-dashed line* = 2σ uncertainty in long-term instrument characterization. *Dotted line* = predicted irradiance variation using Mg II index and scale factors.

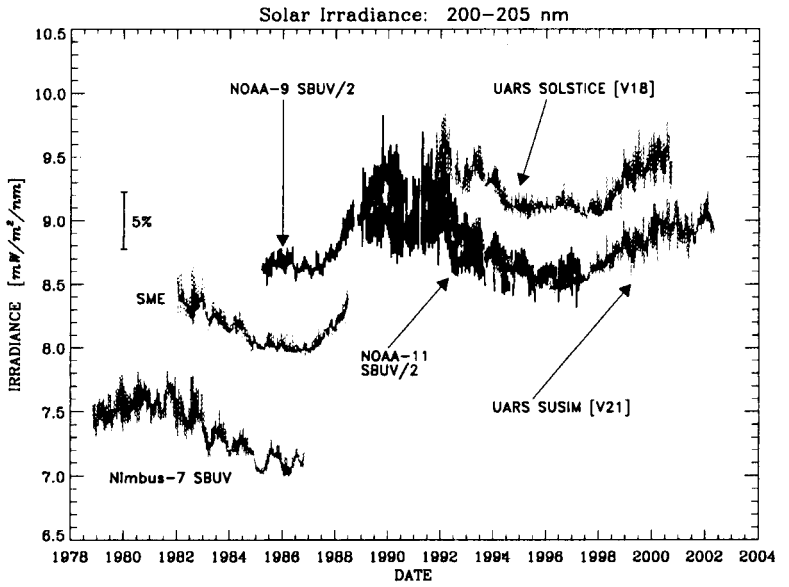

Figure 15. Time series of published solar irradiance data sets at 200-205 nm.

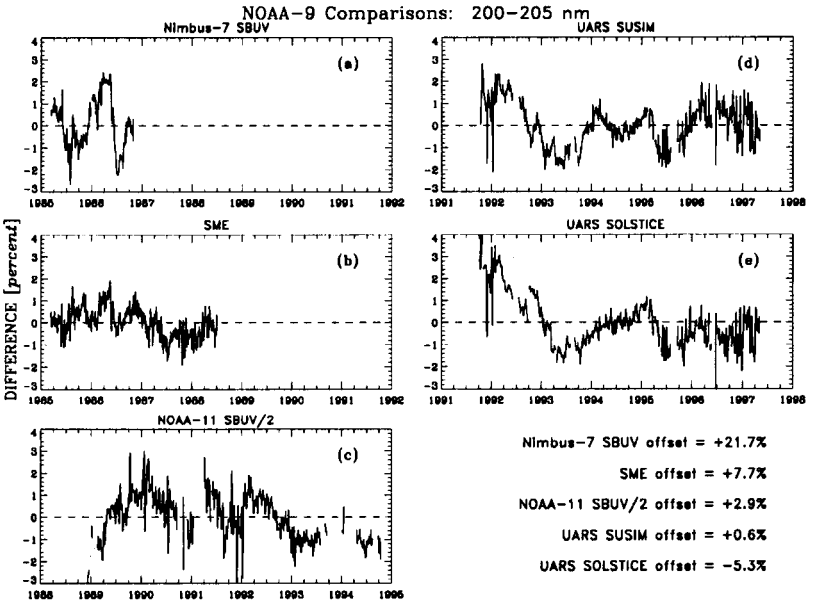

Figure 16. (a) Difference between NOAA-9 SBUV/2 and Nimbus-7 SBUV 200-205 nm data during overlap period. The average bias has been removed. (b) Difference between NOAA-9 SBUV/2 and SME 200-205 nm data during overlap period. (c) Difference between NOAA-9 SBUV/2 and NOAA-11 SBUV/2 200-205 nm data during overlap period. (d) Difference between NOAA-9 SBUV/2 and UARS SUSIM 200-205 nm data during overlap period. (e) Difference between NOAA-9 SBUV/2 and UARS SOLSTICE 200-205 nm data during overlap period.